

## Reversal of bacterial locomotion at an obstacle

Luis Cisneros,<sup>1</sup> Christopher Dombrowski,<sup>1</sup> Raymond E. Goldstein,<sup>1,2,3</sup> and John O. Kessler<sup>1</sup>

<sup>1</sup>Department of Physics, University of Arizona, Tucson, Arizona 85721, USA

<sup>2</sup>Program in Applied Mathematics, University of Arizona, Tucson, Arizona 85721, USA

<sup>3</sup>BIO5 Institute, University of Arizona, Tucson, Arizona 85721, USA

(Received 14 January 2006; published 14 March 2006)

Recent experiments have shown large-scale dynamic coherence in suspensions of the bacterium *B. subtilis*, characterized by *quorum polarity*, collective parallel swimming of cells. To probe mechanisms leading to this, we study the response of individual cells to steric stress, and find that they can reverse swimming direction at spatial constrictions without turning the cell body. The consequences of this propensity to flip the flagella are quantified by measurements of the inward and outward swimming velocities, whose asymptotic values far from the constriction show near perfect symmetry, implying that “forwards” and “backwards” are dynamically indistinguishable, as with *E. coli*.

DOI: 10.1103/PhysRevE.73.030901

PACS number(s): 87.17.Jj, 87.18.Hf, 47.63.Gd

A growing body of work has addressed the spontaneous development of collective patterns by self-propelled organisms [1]. Based on analogies with phase transitions of liquid crystalline and spin systems, phenomenological models [2–4] suggested there could be a transition to a state with long-range order of swimming orientation. Instead, experiments on *E. coli* in suspended soap films [5] and *B. subtilis* in fluid drops [6–8] have shown transient, recurring jets and vortices which disrupt that putative long-range order. Extensions of those models to include hydrodynamic interactions between swimming cells [9,10] and recent numerical studies of large numbers of hydrodynamically interacting force dipoles [11] strongly support the conjecture [7] that such interactions are responsible for these coherent structures.

By itself, steric repulsion of nearly close-packed rodlike cells can produce nonpolar populations: cell bodies aligned as in a nematic liquid crystal. Unidirectional collective swimming requires *polar* alignment, which we term “quorum polarity”; all cells locomoting in the same direction. Because of the rapid, uniform collective velocity of these aligned domains, we call this the “Zooming BioNematic” (ZBN). The search for mechanisms generating quorum polarity served as motivation for the present work. We ask: What happens when the locomotion of a bacterium is impeded by an obstacle? The obstacle might be a wall, another cell or group of cells, perhaps swimming oppositely along a collision trajectory.

Quantitative visualization of the behavior of individual cells is not yet possible in the setting of collective dynamics. Accordingly, we constructed a model experiment to investigate the possibility that hydrodynamic or mechanical stress can cause spontaneous reversal of swimming direction, a mechanism for “wrong way” oriented individuals, hemmed in by neighbors, to join the majority of oppositely directed swimmers, without having to change orientation of the cell body. A reversal entails flipping the bundle of propelling flagella from the original “rear” of the cell to reconstitute at the former “front” end, which becomes the new “rear.” Such a process can provide quorum polarity and can recruit new members to the transient, recurring phalanxes of swimming cells in the ZBN. Such reversals are most properly associated

with peritrichously flagellated cells (those covered with numerous flagella). This paper is devoted to *B. subtilis*; our preliminary studies show that *E. coli* also reverses at obstacles, but less frequently.

Figure 1(a) depicts the experiment, in which macroscopic glass spheres (Sigma-Aldrich, G1152;  $\sim 800\ \mu\text{m}$ ) lie at the bottom of a 1-ml drop of bacterial suspension, 2 cm in diameter, placed on the upper surface of a polystyrene Petri dish. Experiments were conducted on *B. subtilis* strain

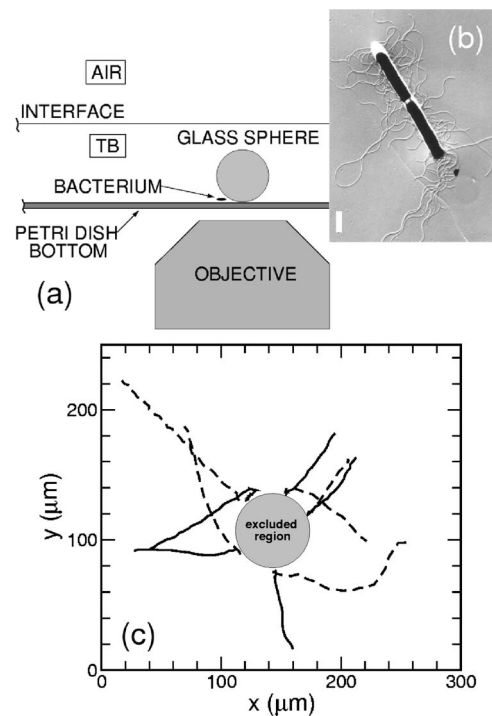


FIG. 1. Apparatus and examples of swimming reversals. (a) A glass sphere at the bottom of a sessile drop (not to scale) of bacterial suspension (Terrific Broth, TB). (b) Electron micrograph of *B. subtilis* about to divide into two cells. The scale bar is  $1\ \mu\text{m}$ . (c) A few incoming (solid) and outgoing (dashed) trajectories at the footprint of an  $800\text{-}\mu\text{m}$ -diam glass sphere.

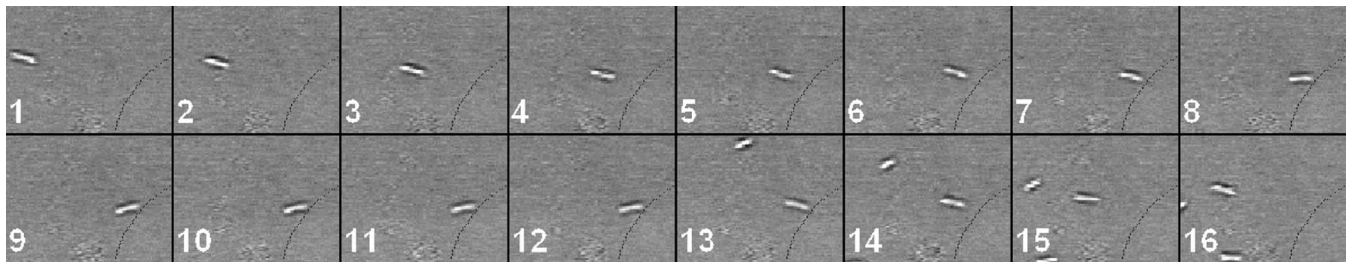


FIG. 2. A bacterial reversal. Images taken 0.28 s apart show a bacterium approaching the narrow gap between a glass sphere and Petri dish, pausing, then swimming back out without turning around. Interlopers seen in frames 13–16 do not affect the motion of the reversing bacterium. The horizontal field of view is  $30\ \mu\text{m}$ . The black arcs mark the radius of closest approach.

1085B, prepared from stock [8]. An electron micrograph [Fig. 1(b)] shows that these cells are  $\sim 4\ \mu\text{m}$  long (considerably longer than *E. coli*) with a very large number of flagella whose length is typically  $5\text{--}10\ \mu\text{m}$ . The sessile drop was obtained from a Terrific Broth (TB, Sigma, T9179) suspension incubated for 3.5 h in a shaker bath, checked for motility, and then diluted 1000-fold with TB. Swimming (Fig. 2) was imaged at  $20\times$  magnification on a Nikon TE2000U inverted microscope with an analog charge-coupled device (CCD) camera (Sony XC-ST50, 30 fps), written to videotape, and digitized for tracking by Metamorph (Universal Imaging Corp.). Additional studies used a high-speed camera (Kodak ES310T, 125 fps).

As the plastic Petri dish is permeable to oxygen, bacteria routinely swim along the bottom of the drop, next to the surface of the dish. *B. subtilis* grown under the conditions described above do not display the classic “run-and-tumble” behavior so well known in *E. coli* [12]. Rather, and especially near a surface, they tend to execute long, perhaps slightly curved swimming trajectories [13,14] with few apparent tumbles. Without direct visualization of flagella, we cannot rule out tumbles with very small angular changes; our observations show that *spontaneous* tumbles with large angular changes in swimming direction are almost entirely absent. Those cells swimming near the bottom occasionally approach the narrow, convex-wedge-shaped gap near the sphere’s contact point, as shown in Fig. 2. Generally, if the angle between their swimming trajectory and the normal to the sphere is large, they simply turn away from the narrowest regions and continue swimming. Relatively straight-on collisions generally produce reversals. An incoming track and its reversed successor is a “V”-shaped pair [Fig. 1(c)]. The video sequences show, without question, that the cell body does not turn around while docked; the forward end of the cell coming into the gap becomes the backward end afterwards; the flagellar bundle flips from one end of the cell to the other. Our findings extend those of Turner and Berg [15], that *E. coli* swims with either end forward. They did not investigate reversal dynamics at obstacles or swimming speed symmetries.

We collected 100 reversal trajectories, five of which are shown in Fig. 1(c). Many display curvature, likely from interaction of the chiral flagellar bundle with the surface, as seen with *E. coli* [13,14]. Using the  $\sim 30\ \mu\text{m}$  radius circle around the sphere’s surface contact point from which bacteria are excluded [Fig. 1(c)], we estimate that reversals occur

at gap heights of  $\sim 1.1\ \mu\text{m}$ , slightly larger than the nominal cell diameter of  $0.7\ \mu\text{m}$ . These cells are covered with flagella and pilli (Fig. 1(b)), so it is plausible that a  $1\text{-}\mu\text{m}$  constriction would stop their motion.

From the full spatial trajectories, we obtained the inward and outward velocities as a function of time relative to the stopping time  $t_{\text{stop}}$  of the inward motion, and the time  $t_{\text{restart}}$  when outward motion begins again. Normalizing the velocities of inward and outward trajectories by each track’s asymptotic value,  $v_{\text{in}}^{\infty}$  and  $v_{\text{out}}^{\infty}$ , and then averaging all 100 such runs, we obtain the average rescaled inward and outward velocities shown in Figs. 3(a) and 3(b). It is evident that earlier than several seconds before stopping and later than a few seconds after resuming swimming, the velocities are nearly independent of time (and hence of position). The

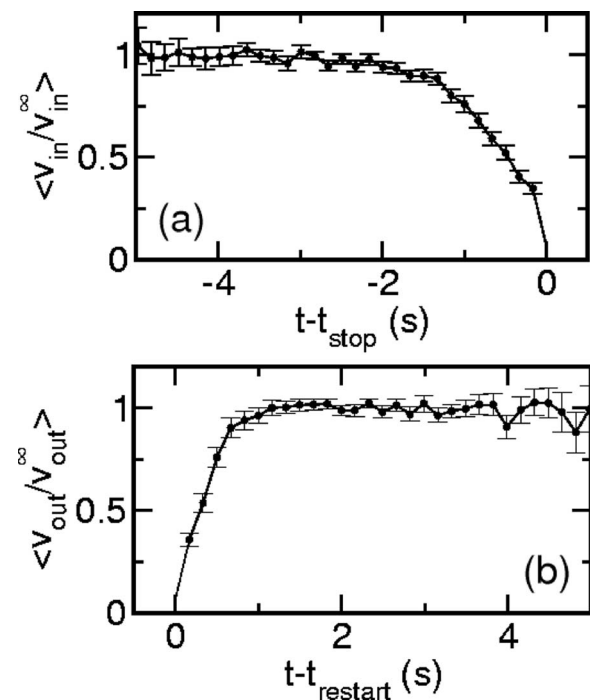


FIG. 3. Time dependence of average swimming velocities. (a) Average of 100 inward tracks, each normalized by the asymptotic velocity far from constriction. (b) As in (a), but for outward tracks. At times larger than shown the statistical uncertainties grow larger due to the fewer number of trajectories in the sample. Uncertainties are standard errors.

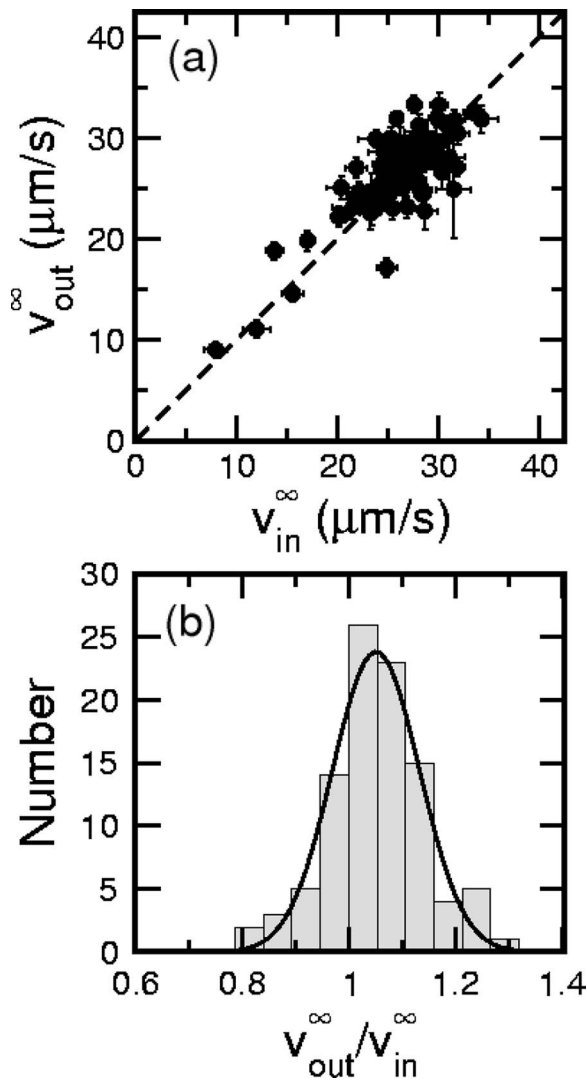


FIG. 4. Statistical results for 100 reversals. (a) Asymptotic outward vs inward velocities, showing tight clustering around line of equalities (dashed). Uncertainties are standard errors. (b) Histogram of asymptotic velocity ratio, with Gaussian fit.

distances associated with these transition times are approximately  $10\text{--}20\ \mu\text{m}$ .

Figure 4(a) shows the asymptotic outward and inward velocities. Over a range from  $\sim 10\text{--}30\ \mu\text{m/s}$  the data cluster near the line of equality. A least-squares fit forced through the origin yields a slope of  $1.01 \pm 0.01$ , showing statistical symmetry. A histogram [Fig. 4(b)] of the ratio  $v_{out}^{\infty}/v_{in}^{\infty}$  shows a Gaussian distribution with a mean of 1.05 and a width of 0.11, again indicating near statistical equality. We infer that swimming ability is independent of the polar location of the flagellar bundle.

As bacteria swim into the gap they experience ever-increasing viscous drag [16] due to the looming proximity of the surface of the sphere. They decelerate to rest on a time scale of  $\sim 2$  s. Following a reversal, the acceleration time scale is more rapid, about 1 s. This asymmetry is easily seen in the temporal traces in Fig. 3 and is further quantified in Fig. 5 as histograms of stopping and starting intervals  $\tau_{stop}$  and  $\tau_{start}$  and the accelerations deduced from them as  $a_i$

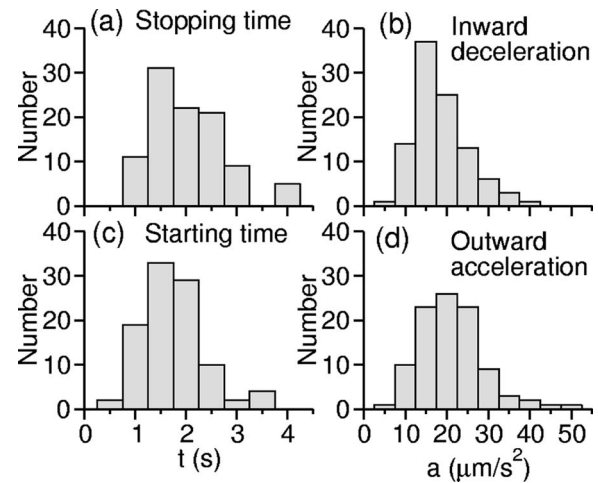


FIG. 5. Statistical analysis of accelerations and decelerations during reversals. Histograms are for the time to decelerate to rest from a steady velocity far away from the wedge on an incoming trajectory, and the time to accelerate from rest to the asymptotic velocity. The average decelerations (accelerations) deduced from those times and velocities are shown.

$=v_{in}^{\infty}/\tau_{stop}$  and  $a_o=v_{out}^{\infty}/\tau_{start}$ . The stopping intervals have a greater mean value than the starting intervals, and the accelerations are also larger than the decelerations.

We interpret these results as a consequence of the different position of the flagellar bundle in the two cases. During inward trajectories, the bundle behind the cell points out into the wider region of the wedge, while during an outward trajectory that bundle, again behind the cell, points into the narrowest regions of the wedge close to the point of contact of the sphere with the substrate. These two orientations differ in viscous drag and propulsive efficiency. Just the opposite asymmetry is observed during tumbles in free-swimming *E. coli* [12]: abrupt deceleration followed by more gradual acceleration as the bundle reforms. Monotrichously flagellated organisms (with a single flagellum) such as *Vibrio alginolyticus*, display similar behavior to that found here: reversals of trajectories without cell reversal, asymptotic equality of speeds far from an obstacle, and asymmetry close in [17].

The time spent “docked” may vary from a few milliseconds to a few seconds, as summarized in the histogram of Fig. 6, from which we deduce that the mean time parked in the wedge is  $\sim 1$  s. It is also evident that reversals occur very quickly, indicating that the typical rebundling time of flagella may be shorter than the time resolution of our imaging process. The incoming and outgoing trajectories define an angle  $\Delta\theta$ , the distribution of which is shown in the top inset of Fig. 6. The angle is broadly distributed and shows no particular correlation with the docking interval itself, indicating that the observed “pivoting” of the docked cell is random. It is important to note that this is true even for very fast reversals, where the range of  $\Delta\theta$  is surprisingly large and there is very little time to pivot. This may prove that the randomness observed does not necessarily come only from some kind of “angular wandering” of the docked cell, but also from details on the unbundling–rebundling process. Dynamical minutiae of reversals will be different in each case, leading to a wide

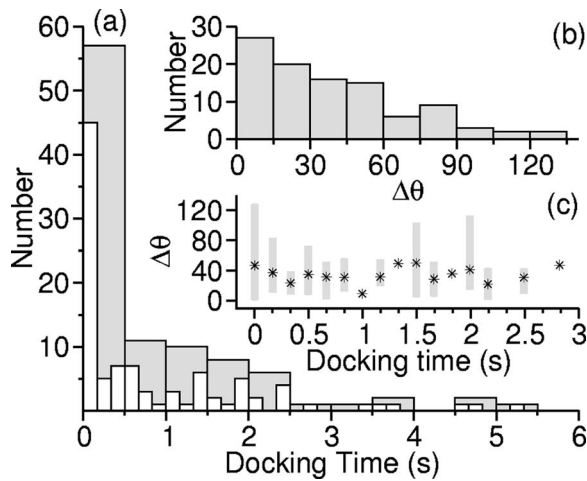


FIG. 6. Statistical analysis of docking. The main figure shows a histogram of docking times with two binning choices. The insets show histograms of the angle  $\Delta\theta$  between in and out trajectories, and a correlation plot between those angles and the docking times. The gray bars indicate maxima and minima observed within each bin, not statistical uncertainties.

distribution of final orientations of the cell. Without direct visualization of flagella [18], we do not know when rebounding completes during a reversal.

It is remarkable that such a major morphological transition as flipping the flagellar bundle appears not to entail consequences beyond swimming at normal speed in the opposite direction. There is a further reversal of symmetry. During

smooth forward locomotion, all the flagella rotate clockwise, as seen from the cell body, at typically 100 turns/s. The cell body rotates appropriately to balance torques. When a swimming cell reverses direction by flipping its flagella, the rotation of its flagella and body reverses *relative* to an observer in the laboratory. When the reversing cell interacts with a domain of the ZBN, the laboratory frame is defined by the director axis, which points along the collectively determined velocity, and by the collectively driven rotation of the fluid. Consider a concentrated population of cells swimming in a particular direction, as in the ZBN. When a “wrong way” swimmer reverses within a phalanx, it changes from contrarotation to corotation relative to its surround. The relative rotation of neighboring cells produces flows orthogonal to the main direction of collective locomotion. In the gap between them, contrarotating neighbors generate microflows of order  $100 \mu\text{m/s}$ . Corotating neighbors produce strong *shear* rates of order  $100 \text{ s}^{-1}$ , estimated by considering flagellar bundles of diameter  $\sim 1 \mu\text{m}$ , rotating at rates of  $\sim 100 \text{ rps}$ , separated by  $\sim 1 \mu\text{m}$ . Shears of this magnitude in the noisy dynamics of the ZBN are ideal generators of flows which enhance mixing, as in the dynamics of blinking stokeslets [19]. Especially significant is improved intercellular signaling, as required for quorum sensing.

We thank Koen Visscher for discussions and D. Bentley for assistance with the micrograph in Fig. 1. This work was supported in part by NSF Grant Nos. MCB-0210854 and PHY0551742, and NIH Grant No. R01 GM72004-01.

- 
- [1] J. Toner, Y. H. Tu, and S. Ramaswamy, *Ann. Phys.* **318**, 170 (2005).  
 [2] J. Toner and Y. Tu, *Phys. Rev. Lett.* **75**, 4326 (1995).  
 [3] T. Vicsek, A. Czirok, E. Ben-Jacob, I. Cohen, and O. Shochet, *Phys. Rev. Lett.* **75**, 1226 (1995).  
 [4] A. Czirok, A.-L. Barabási, and T. Vicsek, *Phys. Rev. Lett.* **82**, 209 (1999).  
 [5] X.-L. Wu and A. Libchaber, *Phys. Rev. Lett.* **84**, 3017 (2000).  
 [6] N. H. Mendelson and J. Lega, *J. Bacteriol.* **181**, 600 (1999).  
 [7] C. Dombrowski, L. Cisneros, S. Chatkaew, R. E. Goldstein, and J. O. Kessler, *Phys. Rev. Lett.* **93**, 098103 (2004).  
 [8] I. Tuval, L. Cisneros, C. Dombrowski, C. W. Wolgemuth, J. O. Kessler, and R. E. Goldstein, *Proc. Natl. Acad. Sci. U.S.A.* **102**, 2277 (2005).  
 [9] R. A. Simha and S. Ramaswamy, *Phys. Rev. Lett.* **89**, 058101 (2002).  
 [10] Y. Hatwalne, S. Ramaswamy, M. Rao, and R. A. Simha, *Phys. Rev. Lett.* **92**, 118101 (2004).  
 [11] J. P. Hernandez-Ortiz, C. G. Stoltz, and M. D. Graham, *Phys. Rev. Lett.* **95**, 204501 (2005).  
 [12] H. C. Berg and D. A. Brown, *Nature (London)* **239**, 500 (1972).  
 [13] W. R. DiLuzio, L. Turner, M. Mayer, P. Garstecki, D. B. Weibel, H. C. Berg, and G. M. Whitesides, *Nature (London)* **435**, 1271 (2005).  
 [14] E. Lauga, W. R. DiLuzio, G. M. Whitesides, and H. A. Stone, *Biophys. J.* **90**, 400 (2006).  
 [15] L. Turner and H. C. Berg, *Proc. Natl. Acad. Sci. U.S.A.* **92**, 477 (1995).  
 [16] H. Brenner, *Chem. Eng. Sci.* **16**, 242 (1961).  
 [17] Y. Magariyama *et al.*, *Biophys. J.* **88**, 3648 (2005).  
 [18] L. Turner, W. S. Ryu, and H. C. Berg, *J. Bacteriol.* **182**, 2793 (2000).  
 [19] H. Aref, *J. Fluid Mech.* **143**, 1 (1984).